BUBBLE NUCLEATION FROM HEATED GLASS CAVITIES

Joel Richard Schapira

NAVAL POSTGRADUATE SCHOOL
Monterey, California

THESIS

BUBBLE NUCLEATION FROM

HEATED GLASS CAVITIES

by

Joel Richard Schapira

Thesis Advisor: P. J. Marto

June 1972

Bubble Nucleation from

Heated Glass Cavities

by

Joel Richard Schapira
Ensign, United States Navy
B.M.E., The Georgia Institute of Technology, 1971

Submitted in partial fulfillment of the
requirements for the degree of

MASTER OF SCIENCE IN MECHANICAL ENGINEERING

from the

NAVAL POSTGRADUATE SCHOOL
June 1972

ABSTRACT

The behavior of bubbles nucleating from a glass cavity was studied using high speed photography. Water and ethanol were used with varying amounts of cavity heat at several subatmospheric pressures.

Bubble growth, departure diameter, and frequency were found to depend on the fluid used, cavity heat, operating pressure and local convection currents. At low pressures, the departure diameter was strongly dependent on dynamic effects. This dependence affected the frequency-departure diameter product such that, contrary to previous high-pressure results, departure diameter increased with increasing bubble frequency.

TABLE OF CONTENTS

LIST OF TABLES

LIST OF FIGURES

NOMENCLATURE

Symbol	Definition
D	Diameter
d	Measured bubble diameter
f	Bubble frequency
g	Gravitational acceleration
h	Convective heat transfer coefficient
L	Latent heat of vaporization
R	Bubble radius
T	Temperature
t	Time
V	Volume
x	Measured bubble height

Subscripts

c	Cavity
d	Departure
L	Liquid
o	Mean bulk
s	Equivalent spherical
v	Vapor

ACKNOWLEDGEMENTS

The author would like to express his thanks to Dr. Paul J. Marto of the Naval Postgraduate School for his suggestions and enthusiastic support during this study.

Mr. Robert C. Sheile, also of the Naval Postgraduate School, constructed the glass apparatus used in this study. His expertise and constant helpfulness are greatly appreciated.

I. INTRODUCTION

With advances in technology, the desire to transfer larger amounts of heat over smaller areas has steadily increased. This desire has rather naturally lead to boiling heat transfer, a process involving phase changes and large scale fluid motions. While boiling has become an increasingly important mode of heat transfer, it is one of the least understood heat transfer phenomena.

The life of a bubble in nucleate boiling may be roughly divided into two regions. The first portion of a bubble's life is spent attached to some surface. The bubble enters its second phase of life when it separates from the surface. The concern in this work is with the bubble prior to separation.

The problems of bubble growth, bubble departure diameters, and bubble frequencies have been studied by many investigators. The vast bulk of the investigations on bubble behavior has been carried out for boiling from heated strips: Staniszewski [1] and Cole [2]. Zuber [3] considered the problem of a bubble growing from an orifice. More recently DuBois [4] and Sowersby [5] have performed experiments to study bubble behavior for bubbles nucleating from glass cavities at atmospheric and slightly reduced pressures.

It was the purpose of this thesis to investigate bubble behavior for bubbles nucleating from a glass cavity. Heat supplied directly to the cavity, fluids, and operating pressures were to be varied in this study. Particular attention was to be paid to bubble behavior at low pressures.

II. EQUIPMENT AND PROCEDURES

A. EQUIPMENT

The central piece of apparatus used in the experimental runs was the glass cavity from which boiling was observed. The cavity, as shown in Fig. 1, was mounted on a Pyrex tube, which, in turn, was mounted on a ground glass socket joint. A small cavity heater was then mounted within the Pyrex tube and against the cavity bottom. Appendix A describes the cavity, heater, and their construction.

The cavity assembly was inserted through the bottom of the boiler and secured with a ball-and-socket joint clamp. Figures 2 and 3 illustrate the boiler with a cavity in place. The boiler was approximately nine inches high with an outer diameter of five inches. To facilitate a photographic examination of the cavity, with minimum distortion, a two-inch diameter flat glass window was mounted approximately half way up the side of the boiler. Topping the boiler was a removable glass dome. The top was made removable to ease boiler cleaning and filling. Fitted onto the top were two glass receptacles for removable thermocouple wells and a valve through which a vacuum could be drawn and secured.

Surrounding the inner boiler was an oil jacket. The oil jacket was used to supply heat to the boiler in a manner by which convection currents within the boiler could be minimized and to insulate the boiler from ambient conditions. In conjunction with the photographic study, a glass window, similar to the boiler window, was mounted on the side of the oil jacket and parallel to the boiler window. During all operations, the oil jacket was vented to the atmosphere through

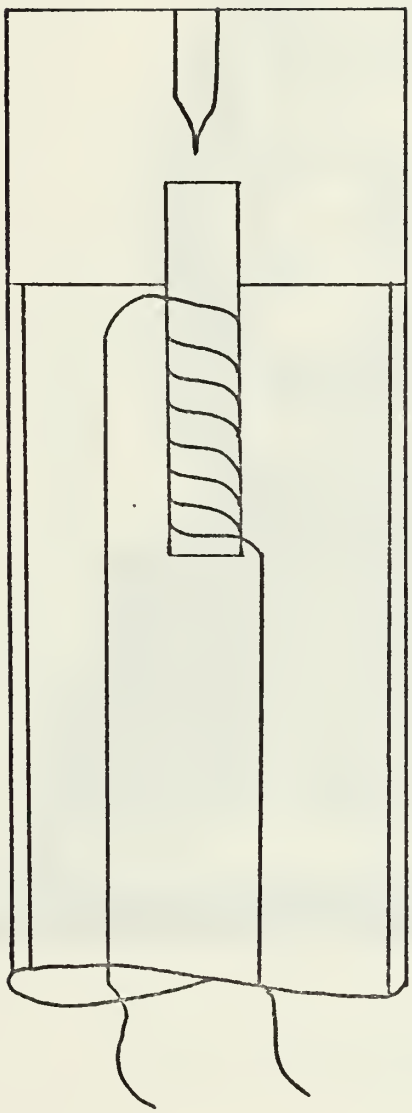

Cavity Diameter
0.021 in
Cavity Depth
0.147 in
Assembly OD
.290 in.

Fig. 1. Cavity and Heater

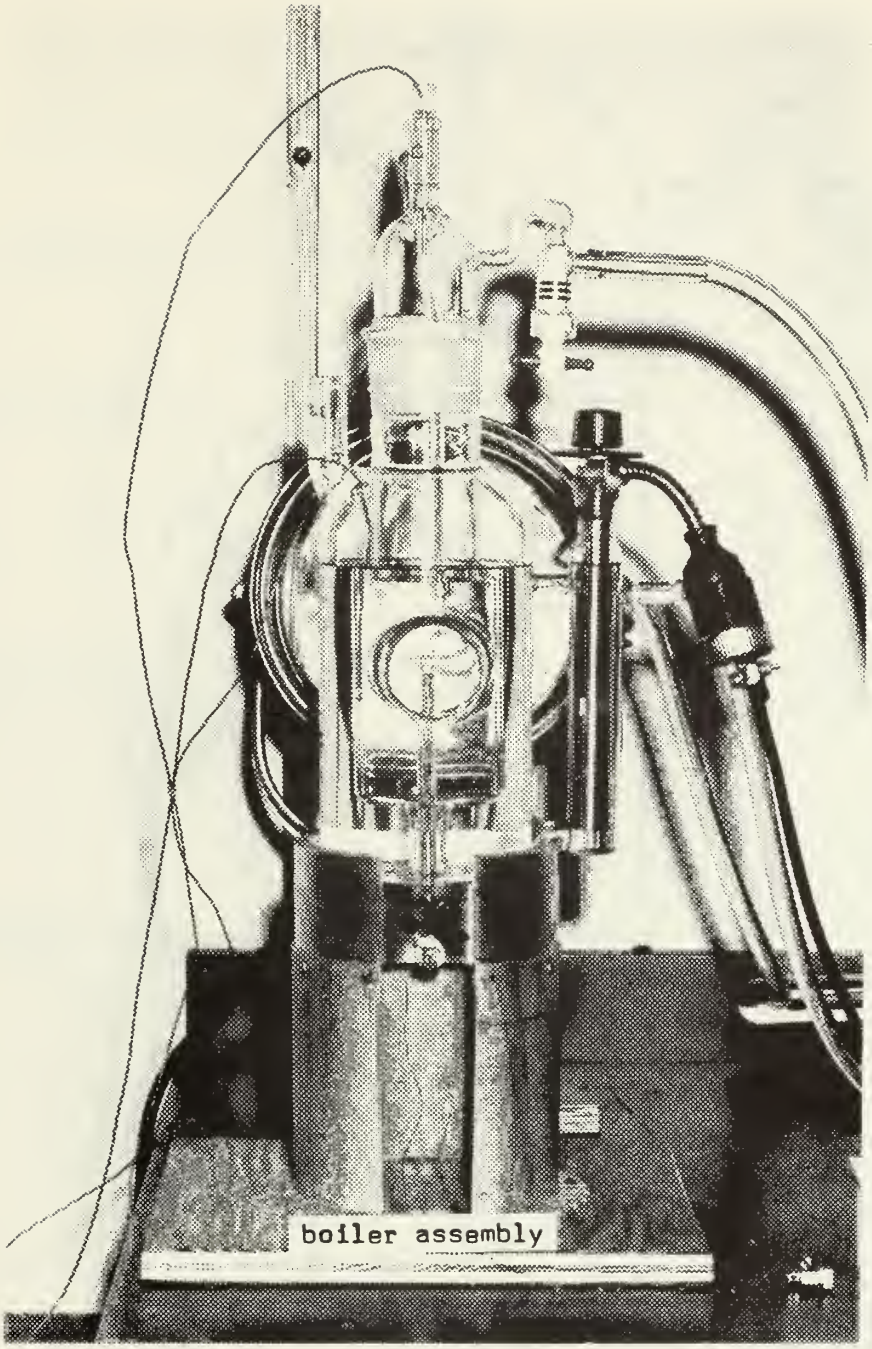

Fig. 2. Boiler Assembly

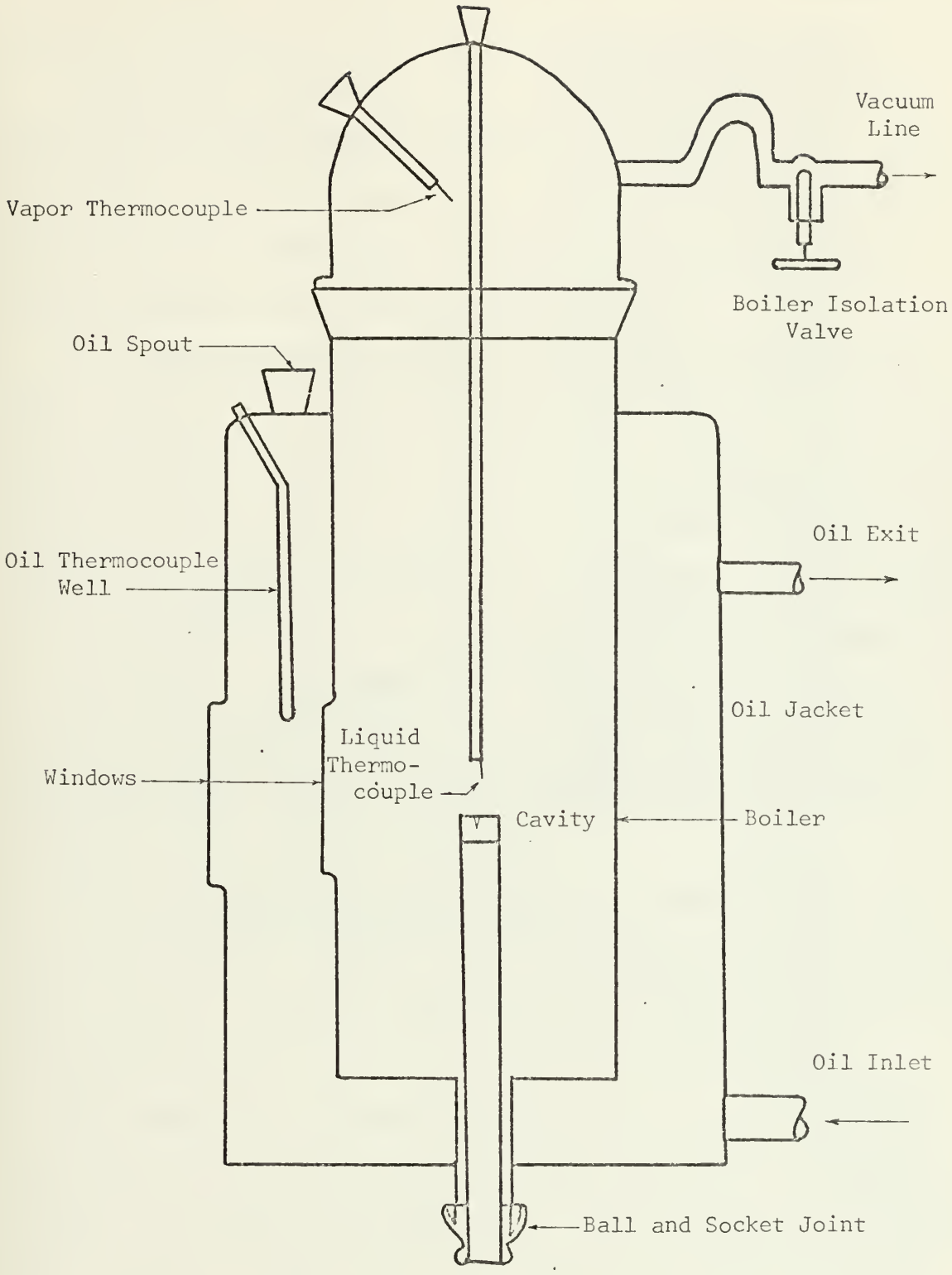

Fig. 3. Boiler and Cavity

the filling port. Dow Corning Type 200 Silicone Oil was circulated through the jacket via a lower inlet port and an upper exit port.

During an oil cycle Fig. 4, the oil would flow from the jacket and through a single pass, tube-in-tube heat exchanger. Upon exiting the heater, the oil was pumped over a Fenwell All Purpose Thermoswitch and into the oil jacket inlet. A Variac controlled, Jabsco self-priming pump was used to circulate the heated oil.

The tube-in-tube heat exchanger, or oil heater was constructed from a 20 inch, 1 1/4 inch OD Pyrex tube into which a smaller concentric tube was mounted. The heater, a 16 inch long nichrome coil, was placed inside the inner glass tube. Power to the oil heater was supplied and regulated by a Variac. The thermoswitch was mounted in series with the heater and Variac and set to maintain a pre-determined oil temperature.

In many of the experimental runs, additional heat was supplied with the cavity heater. The small power levels to the cavity heater were supplied and regulated through a Lambda LK 345A FM D.C. power source.

The vacuum system consisted of a cold trap protected vacuum pump and a Kinney Measuvac pressure gage connected with tubing to the boiler top. In order to minimize vacuum leakage during operation, all of the glass joints in the boiler top were fitted with Teflon sleeves.

The temperature instrumentation attached to the boiler assembly consisted of three copper-constantan thermocouples. Two of the thermocouples were mounted through glass wells which were placed in the boiler top. The boiler thermocouples, one of which was positioned in the vapor space, the second in the liquid, were bare junction type. The third thermocouple was placed within a glass well in the oil jacket.

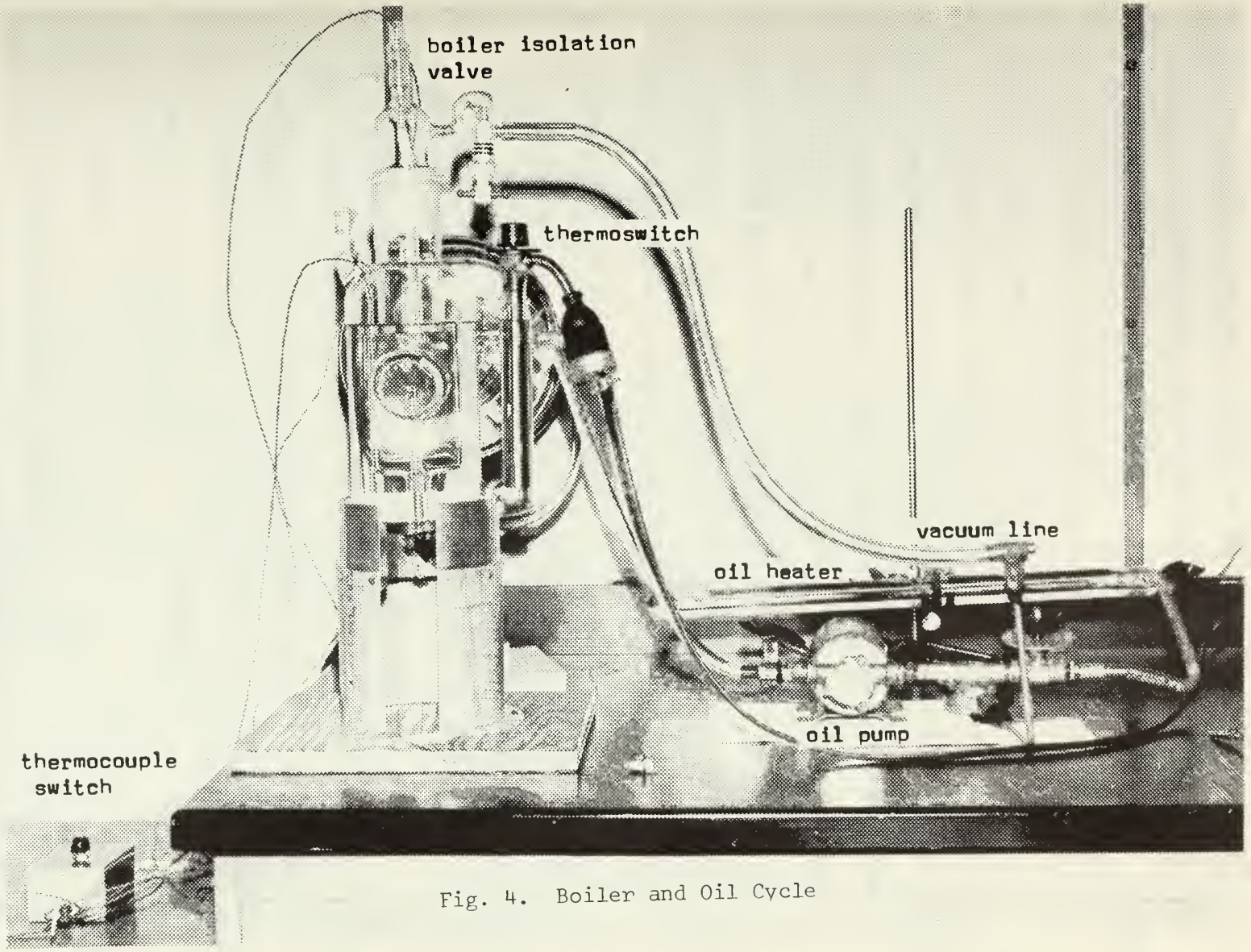

Fig. 4. Boiler and Oil Cycle

All of the thermocouples were connected to a switch which connected each thermocouple to an ice junction for individual thermocouple readings and bucked the boiler thermocouples against each other for a determination of local superheat near the glass cavity. The output from the thermocouple switch was then read on a Leeds and Northrup millivolt potentiometer.

A Fairchild Model HS401 Motion Analysis Camera was used to take high speed motion pictures of bubbles nucleating from the glass cavities. The motion pictures were taken through the parallel glass windows on the oil jacket and boiler. The camera, equipped with motors for a nominal film speed of 4800 frames per second, was powered through a Fairchild Model HS-5105B Motor Control. Direct illumination for filming was provided by a Variac controlled Colortran Light Fixture with a 1000 watt floodlight.

Filming of experimental runs was made using Eastman 4-X, 16 mm, Panchromatic Negative Film and Tri-X, Panchromatic Reversal Film. To enable the camera to attain a steady speed before actual filming, a 300 or 200 foot leader of developed film was spliced to 100 or 200 foot length of unexposed film for each 400 foot reel. Timing tics were placed on the film by using a General Radio Company, Strobotac Type 1531A strobe operated at 200 flashes per second. Figures 5 and 6 illustrate the relative layout of the equipment.

B. PROCEDURE

1. Preparation of Test Apparatus

Prior to each series of experimental runs, the boiler was thoroughly cleaned with concentrated chromic acid and rinsed with distilled water. The purpose of the boiler cleaning was to promote

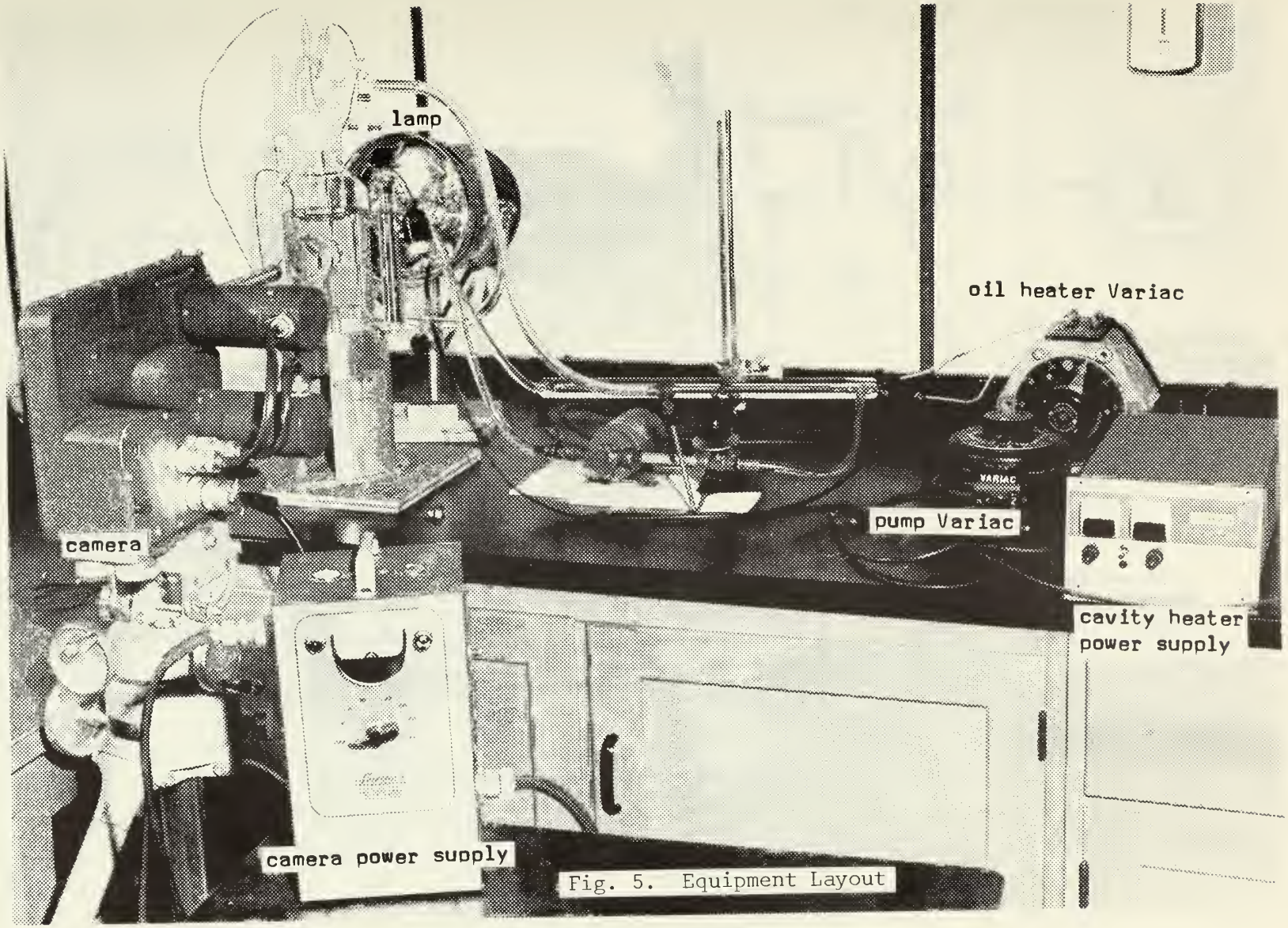

Fig. 5. Equipment Layout

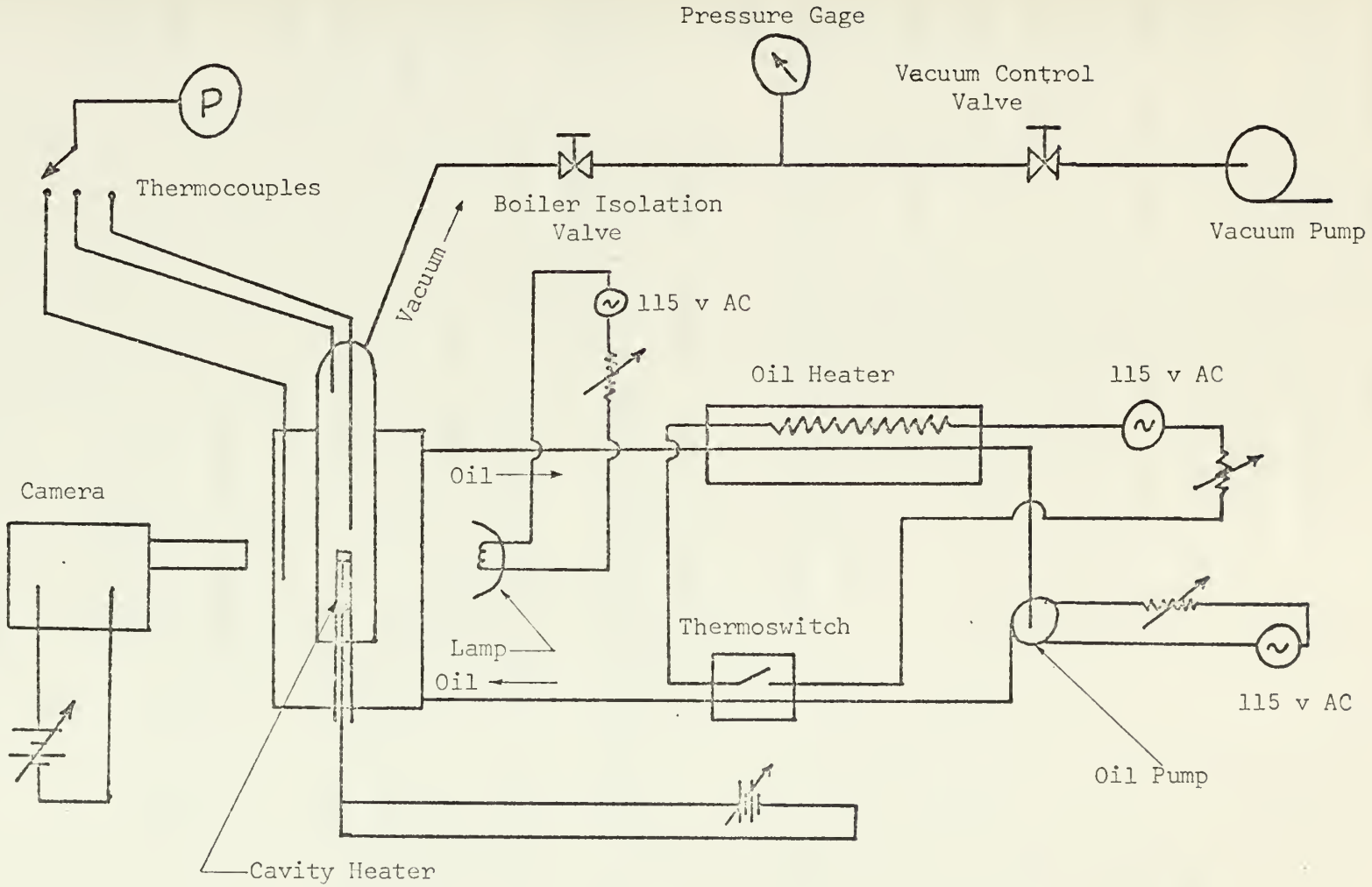

Fig. 6. Schematic of Equipment

liquid wetting within the boiler, thereby suppressing unwanted nucleation sites on the boiler walls. For both the water and ethanol runs, this method of boiler cleaning was found to be quite satisfactory.

The procedure for cleaning the glass cavity differed slightly from the procedure used to clean the boiler. The cavity and supporting tube were soaked and scrubbed in warm concentrated commercial glass detergent. The cavity assembly was then rinsed with distilled water and soaked in a concentrated sodium hydroxide solution. Following a water rinse, the assembly was soaked in concentrated chromic acid. After another water wash, the socket joint on the cavity assembly was coated with Dow Corning High Vacuum Grease. Care was taken to prevent the grease from contacting the glass cavity area or the glass supporting rod.

The cavity assembly was then inserted into the boiler. The cavity was rotated several times to allow the vacuum grease to properly seal the cavity-boiler joint.

With the cavity in place, the cavity heater was activated and a vacuum drawn on the empty boiler. The purpose of this procedure was to remove any liquid still in the cavity. Once the cavity interior was dry, as optically determined, the cavity heat was turned off and the boiler returned to atmospheric pressure.

With the boiler at atmospheric pressure, the boiling fluid was poured through the vapor thermocouple port. The liquid level was brought to about one inch over the cavity top.

2. Experimental Procedure

With the boiler filled and all thermocouples in place, a vacuum was drawn on the boiler, the heating oil was circulated and, if necessary, the oil heater was turned on.

The vacuum was adjusted and maintained by continuously running the vacuum pump. The boiler pressure was monitored with the line pressure gage and controlled with a valve located between the pressure gage and the vacuum pump.

Upon start up, the heating oil was circulated through the oil jacket and oil heater. The rate of oil flow was controlled by varying the speed of the oil circulating pump with a Variac.

Heat was added to the oil in the Variac controlled oil heater. The oil heater was manually adjusted until the boiler reached the desired operating temperature. With the boiler at the desired temperature, the boiler vacuum was adjusted until bubbles were regularly nucleating from the glass cavity. The cavity heat was then adjusted to the desired level. The system was then operated in a steady fashion for five minutes.

During the five minute steadying period, the camera was loaded with film and focussed on the cavity. Any necessary adjustments to the lamp were also made at this time. The lamp's illumination was controlled with a Variac and monitored with a Wollensak light meter. The illumination was adjusted to supply the necessary light for the specific film, camera speed used, and lens opening.

With the camera loaded and adjusted, the camera's power supply was adjusted for the desired camera speed, the lamp illuminated and the film run started.

During film runs, a General Radio Company Strobotac was operated at 200 flashes per second. The strobe was directed through special ports in the camera body and against the edge of the film. The resulting timing tics on the film were used during the analysis of the film to obtain bubble growth-time data.

After a film run, the camera was cleaned of film chips and re-loaded. The boiler conditions were then varied for the next experimental run.

Temperature measurements were taken at regular intervals throughout the experimental runs. In most cases, film runs were not carried out until the vapor thermocouple indicated the saturation temperature corresponding to the vacuum gage pressure. The exception to this procedure occurred with ethanol boiling at medium pressures. The boiler dome acted as a condenser for the ethanol vapors, the level of condensation never reaching the position of the vapor thermocouple. In this case, filming was commenced when a regular stream of bubbles issued from the cavity.

A further difference in the procedure between ethanol and water occurred during heating to desired operating conditions. For ethanol it was necessary to maintain boiling from the cavity as the boiler was heated. If boiling was not maintained, the cavity flooded and could not be re-activated. Boiling was maintained by varying the boiler pressure in order to maintain saturated conditions within the boiler. The only precaution necessary to prevent flooding of the cavity in water was the constant operation of the cavity heater during heating to the desired conditions.

The amounts of cavity heat supplied during runs with cavity heat varied for water and ethanol. The cavity heat supplied to the cavity in water was limited to five watts, the level above which nucleation occurred on the outer walls of the cavity-heater assembly. Cavity heat for ethanol experiments was limited to nine watts by resistive losses in the heater leads. No cases of unwanted nucleation sites were experienced with ethanol.

The conditions under which experimental runs were performed are found in Table I. Physical properties of the fluids used are tabulated in Appendix B.

TABLE I

EXPERIMENTAL CONDITIONS

Fluid	Pressure (in Hg abs)	Cavity Heat	T(Fluid)	T(Vapor)
Water	7.4	0	145.3°F	143.0°F
	6.9	5W	145.8	140.9
Ethanol	5.9	0	108.7	107.0
	5.9	9W	110.9	109.1
	20.4	0	156.2	----
	20.4	9W	157.9	----

3. Data Analysis and Reduction

Other than the data obtained on operating conditions during the experimental runs, the primary data on bubble growth was taken from 16 mm motion picture films. The motion picture films were analyzed with the use of a Kodak Analyst projector. The Kodak projector has a single frame capability and a frame counter to aid in time determinations. For each frame analyzed, the bubble height from the glass cavity and the maximum bubble diameter were measured, as illustrated in Fig. 7. The cavity diameter served as a standard for bubble measurements. Time determinations were made by using the frame counter and a knowledge of the frame separations between timing tics.

An equivalent spherical bubble diameter was calculated for each bubble measurement taken. Cole and Shulman [6] assumed that the bubble

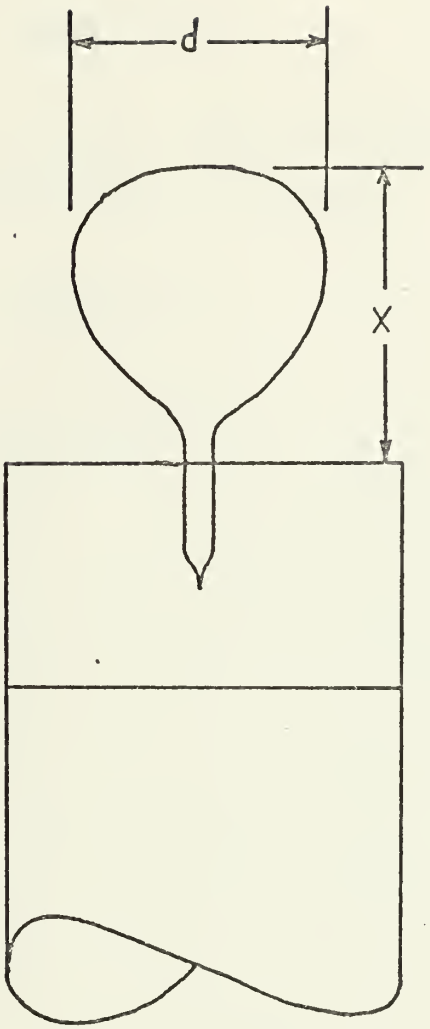

Fig. 7. Bubble Geometry

volume is approximated by an ellipsoid having a diameter equal to the measured bubble diameter, and a major axis equal to the bubble height, or

$$V = \frac{\pi}{6} dx^2,$$

where d = measured bubble diameter

and x = measured bubble height.

An equivalent spherical bubble diameter is defined as the diameter of a sphere having the same volume as a bubble:

$$D = \left(\frac{6}{\pi} V\right)^{1/3}$$

or

$$D_S = \left[dx^2\right]^{1/3} .$$

III. PRESENTATION AND DISCUSSION OF DATA

A. BUBBLE CHARACTERISTICS

The most striking difference between ethanol bubbles at all pressures and water bubbles is the presence of a vapor patch, Fig. 8, atop the glass cavity for water bubbles. The vapor patch was present for all cases of water boiling, despite thorough cleaning procedures and variations in cavity heat. This vapor patch, so persistent for water, was never present for the ethanol experiments. The ethanol, superior to water in wetting, completely wetted the cavity top. The superior wetting characteristics of the ethanol limited the solid-vapor interface to the cavity rim during most portions of bubble growth. Immediately following bubble separation, Fig. 8, the liquid-vapor interface descended into the cavity. As a result of the vapor patch in water experiments, no penetration was possible for water bubbles.

The ethanol bubbles varied in shape with different operating pressures. The low pressure bubbles, as exaggerated below grew in an approximately hemispherical fashion during early growth stages. The medium pressure bubbles rapidly lifted off the cavity surface.

B. GROWTH OF BUBBLES

An examination of the bubble growth curves, as shown as plots of the ratio of equivalent spherical bubble diameter to cavity diameter vs. time in Figs. 9 and 10 seems to indicate a power low dependence of diameter on time. The bubble growth curves were formed by taking two extreme growth curves for bubbles under the same conditions. To aid in the comparison of growth rates, the growth curves for bubbles with cavity heat were plotted on the same graphs as unheated bubbles.

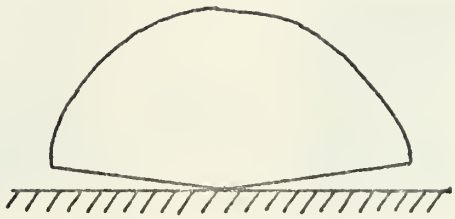

Low Pressure Bubble

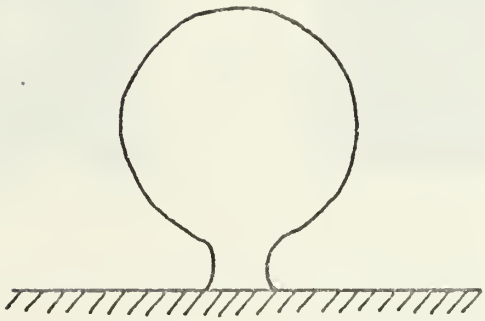

High Pressure Bubble

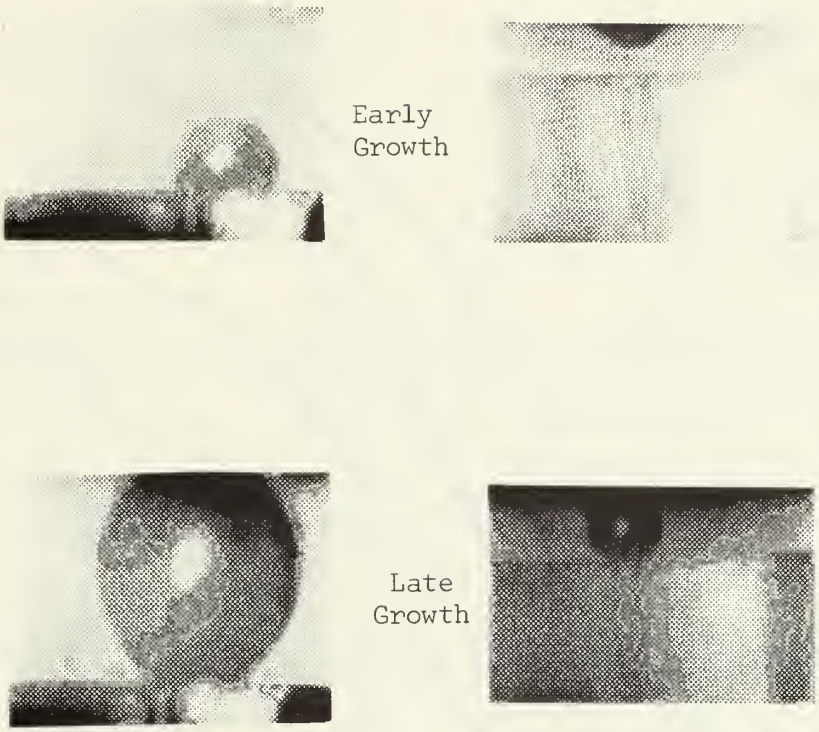

Fig. 8. Cavity Action in Water and Ethanol

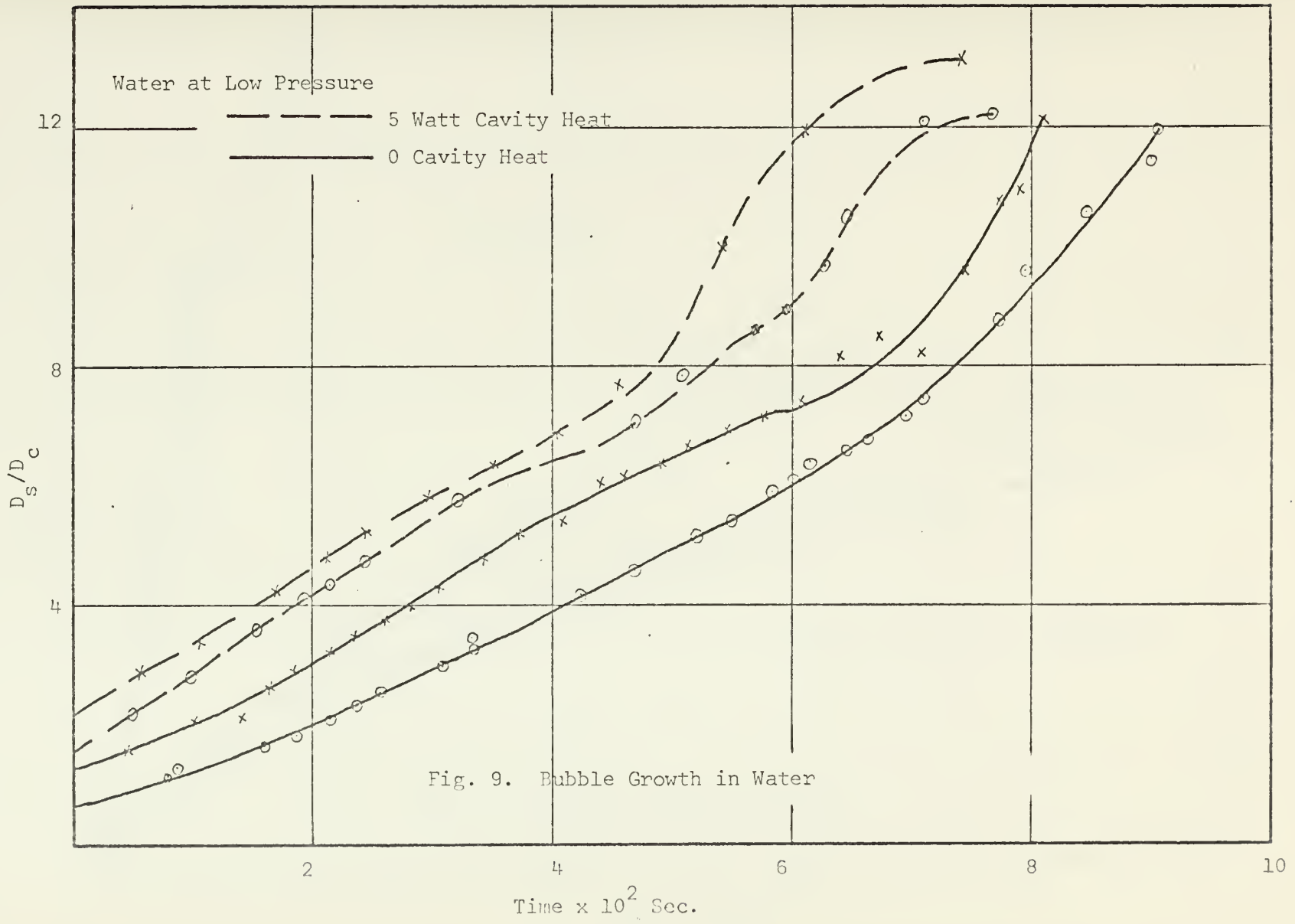

Fig. 9. Bubble Growth in Water

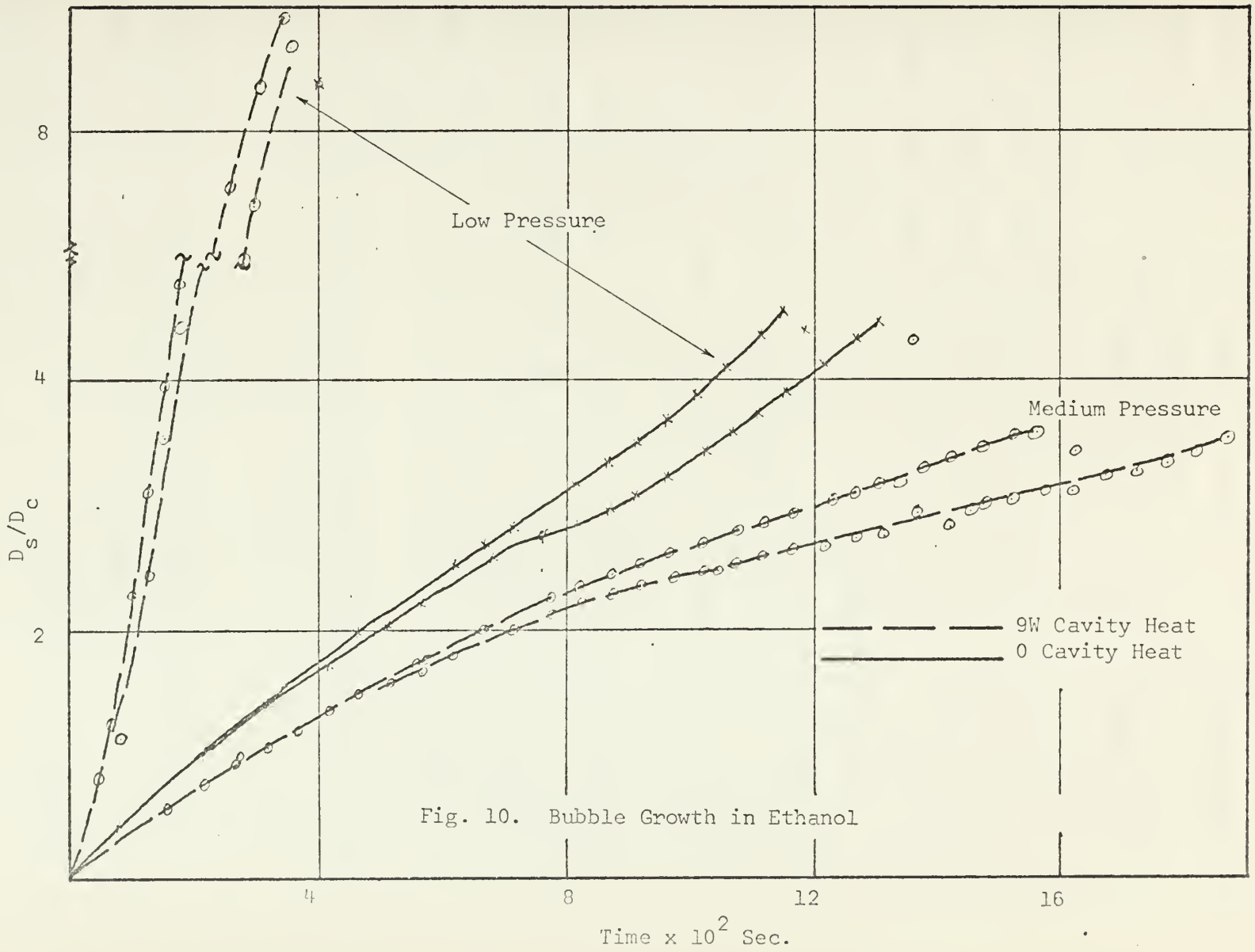

Fig. 10. Bubble Growth in Ethanol

In all of the bubbles studied, the cavity heat markedly increased bubble growth, increased bubble departure diameter, and increased the bubble frequency. The rather odd decrease of the equivalent spherical bubble diameter for the ethanol bubbles prior to departure is due to the manner in which the equivalent spherical bubble diameter was determined. The lengthening of the bubble neck, prior to separation, tends to distort the bubble from an ellipsoidal geometry and to give an erroneously high equivalent spherical bubble diameter. Data for departure diameters were taken just after bubble departure. The recently departed bubbles lacked the errors caused by an elongated neck and did, in fact, resemble ellipsoids. The bubble growth curves for water, Fig. 9, illustrate the effects of the vapor patch surrounding the cavity, Fig. 8. The effects are most clearly seen at the zero time points and the fact that the bubble diameters did not go to zero. To correct for these effects, the zero time points were moved to zero diameters by subtracting the appropriate $\frac{D_s}{D_c}$ at zero time from each curve prior to the log-log plots, Figs. 11 and 12. The wetting action of ethanol prevented similar effects with boiling ethanol and corrections were not necessary.

When log-log plots were made of bubble growth data, Figs. 11 and 12, the bubbles appeared to follow a power law growth of the form

$$D \alpha t^n.$$

The exponent, n, was found to vary with pressure, cavity heat, and specific region of bubble growth as may be seen in Table II.

According to the Plesset- Zwick and Forster-Zuber theories [8,9], bubble growth is of the form

$$R = C\Delta T t^{1/2}$$

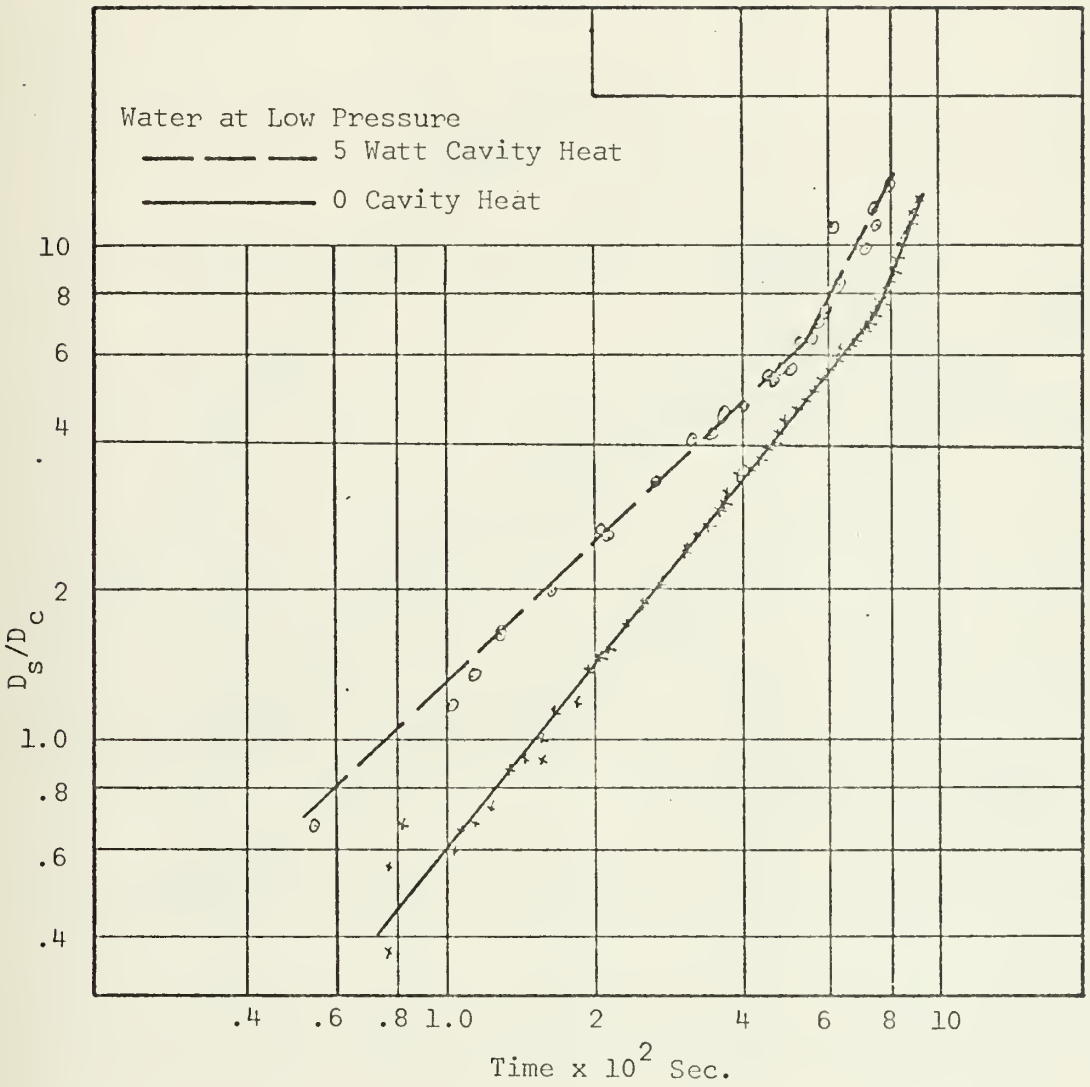

Fig. 11. Water Bubble Growth

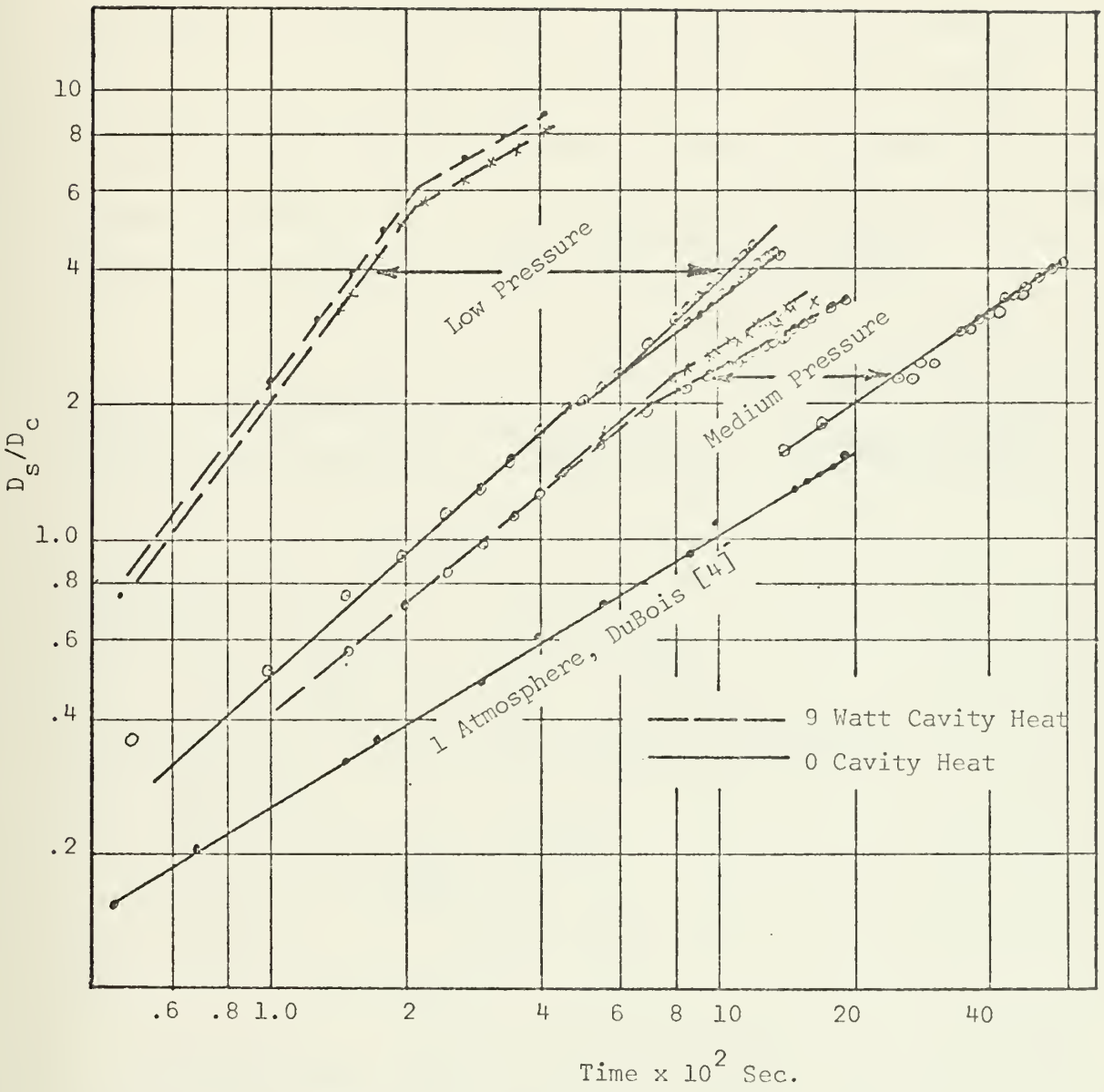

Fig. 12. Ethanol Bubble Growth

Both formulas were obtained through an energy balance describing the heat transfer between a growing bubble and the fluid:

$$h(T_o - T_{sat}) = L\rho_v \frac{dR}{dt} .$$

Zuber [3,10] obtained expressions for R(t) by solving the above equation for constant and non-uniform temperature fields. In each solution, an infinite, stagnant fluid was assumed. It was further assumed that heat transfer through the fluid to the bubble was via conduction which cooled the fluid near the growing bubble. With these assumptions

$$h = k/\delta,$$

where k is the thermal conductivity of the liquid and δ the thermal boundary layer thickness. For conduction in a semi-infinite body,

$$\delta = C_1\sqrt{t},$$

yielding

$$\frac{k}{C_1\sqrt{t}} (T_o - T_{sat}) = L\rho_v \frac{dR}{dt} .$$

With $(T_o - T_{sat})$, or ΔT, at most a function of position,

$$R = \frac{k}{C_1 L\rho_v} \Delta T\, t^{1/2},$$

or

$$R = C\Delta T\, t^{1/2} .$$

Following Zuber's work, Griffith [7] mathematically treated the growth of a hemispherical bubble from a constant temperature plate. Griffith assumed bubble growth to take place into a quiescent fluid with heat conducted through the liquid to the growing bubble. Griffith's numerical solution to this problem was later analyzed by Staniszewski [1], and found to be described by an equation of the form

$$R = Ct^n,$$

n varying with time. During early stages of growth, n was found to be close to 1/2, then decreased to between 0.22 and 0.35. The value of n in the latter stages of growth was dependent upon fluid properties. Staniszewski's [1] experiments for water and for methyl alcohol boiling from a copper strip at atmospheric and elevated pressures yielded n's generally larger than .50 and approaching 1.0 in early stages of growth. During latter stages of growth, Staniszewski's n's decreased to a value of about 1/3.

The power dependence of bubble size on time as determined by the present experiments is significantly larger than that predicted by the theories of Forster-Zuber or Griffith. The primary reason for this discrepancy is felt to be due to the effects of local convection currents set up in the boiler by side and bottom heating. (See Fig. 13.)

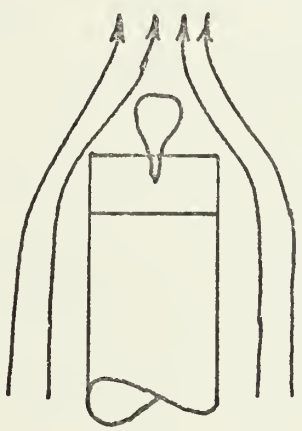

Fig. 13. Cavity Convection Currents

A heat balance on a growing bubble yields:

$$h(T_o - T_{sat}) = L\rho_v \frac{dR}{dt} .$$

If natural convection is assumed in the vicinity of the bubble and if the cooled liquid near the bubble is constantly replaced by warmer fluid, then the left side of the above equation is approximately constant, or

$$R \alpha t.$$

An almost linear dependence of bubble size upon time was found for water boiling at low pressure with cavity heat. Ethanol boiling at low pressure without cavity heat and at medium pressure with cavity heat also demonstrated almost linear behavior. A greater than linear relationship is possible if the fluid being convected past the cavity has a higher degree of superheat than in the local vicinity of the cavity.

A comparison of Figs. 11 and 12 shows that a marked change occurs in the value of n at Ds/Dc ratios between 5.5 and 6.5. It is felt that these abrupt changes in the slope of the log-log growth curves are due to the effects of boiler convection currents, Fig. 13. In the water experiments, the oil jacket was from 11°F to 14°F warmer than the boiler water. For the low pressure ethanol experiments, the reverse case was maintained with the ethanol four to six degrees cooler than the oil. It is felt that cooling currents from the boiler walls depressed the growth rate for low pressure ethanol bubbles with diameter ratios greater than 5.5.

A further point to note on bubble growth is apparent from Table II. The exponent of growth, n, is seen to increase with the addition of

TABLE II

VALUES OF BUBBLE GROWTH EXPONENT

Bubble Conditions	n (initial)	D/D_c at transition	n after transition
Water, Low Pressure			
No Cavity Heat	1.23	6.5 - 7.0	2.35 - 2.40
5W Cavity Heat	0.95	6.5	1.84 - 2.05
Ethanol, Low Pressure			
No Cavity Heat	0.90		
9W Cavity Heat	1.33 - 1.35	5.6 - 6.0	.575
Medium Pressure			
No Cavity Heat	0.685		
9W Cavity Heat	0.84	2.2	.625
Atmospheric Pressure	0.61 (a)		

(a) Data obtained from DuBois [4] for a 0.0395 ID cylindrical cavity.

cavity heat and with a reduction of pressure for ethanol. The fact that this trend was not observed for water at low pressure with the addition of cavity heat was due to the presence of spurious nucleation sites on the heated cavity. Data obtained from DuBois [4] for ethanol boiling from an unheated 0.0395 inch diameter cavity at atmospheric pressure substantiates the trend of n with pressure.

C. DEPARTURE DIAMETERS

Much work has been performed in the study of bubble departure diameters in nucleate boiling. Fritz [11] led the studies with a prediction for departure diameters of static bubbles. Fritz's solution predicts that bubble separation will occur when surface tension forces equal buoyancy forces. This leads to the expression:

$$\sqrt[3]{V_D} = .0119\beta \sqrt{\frac{2g_c\sigma}{g(\rho_L-\rho_V)}} .$$

If a spherical bubble is assumed, this becomes:

$$D_d = .0208\beta \sqrt{\frac{g_c\sigma}{g(\rho_L-\rho_V)}} ,$$

where β is the contact angle in degrees.

Staniszewski altered Fritz's prediction by adding a dynamic dependence to the departure diameter. With Fritz's prediction equated to a D_o, Staniszewski held that

$$D_d = D_o(1 + a\,(\frac{dD}{dt})),$$

"a" being a constant and $\frac{dD}{dt}$ evaluated at separation. For boiling from a horizontal copper strip at from one to two atmospheres, Staniszewski [1] found:

$$D_d = .0071\beta \left(\frac{2g_c\sigma}{g(\rho_L-\rho_V)}\right)^{1/2} \left(1 + .435 \frac{dD}{dt}\right).$$

An analysis of Fig. 14, a plot of the equivalent spherical diameter ratio at departure against the rate of growth at departure leads to:

$$\frac{1}{D_c} D_d = 2.55 + .046 \frac{d}{dt}\left(\frac{D_d}{D_c}\right).$$

When Fritz's solution is extracted,

$$D_d = .625 \sqrt{\frac{2g_c\sigma}{g(\rho_L-\rho_V)}} \left(1 + .855\frac{dD_d}{dt}\right).$$

At reduced pressures, it is therefore found that the dynamic effects on departure diameter are considerably more important than Staniszewski found them to be at atmospheric and increased pressures.

D. FREQUENCY-DEPARTURE DIAMETER RELATIONSHIPS

Much has been written concerning various bubble frequency to departure diameter relationships. Jakob [12] presented data for boiling at atmospheric pressures and noted, over a range of diameters, that the fD_d product was constant. Zuber [3] proposed that the fD_d product was proportional to the bubble rise velocity. Using the results of Peebles and Garber, Zuber found

$$fD_d = 0.59 \left(\frac{\sigma g \Delta\rho}{\rho_L^2}\right)^{1/4}.$$

McFadden and Grassman [13] examined previously published data and their own data for nucleate boiling in liquid nitrogen. They concluded that

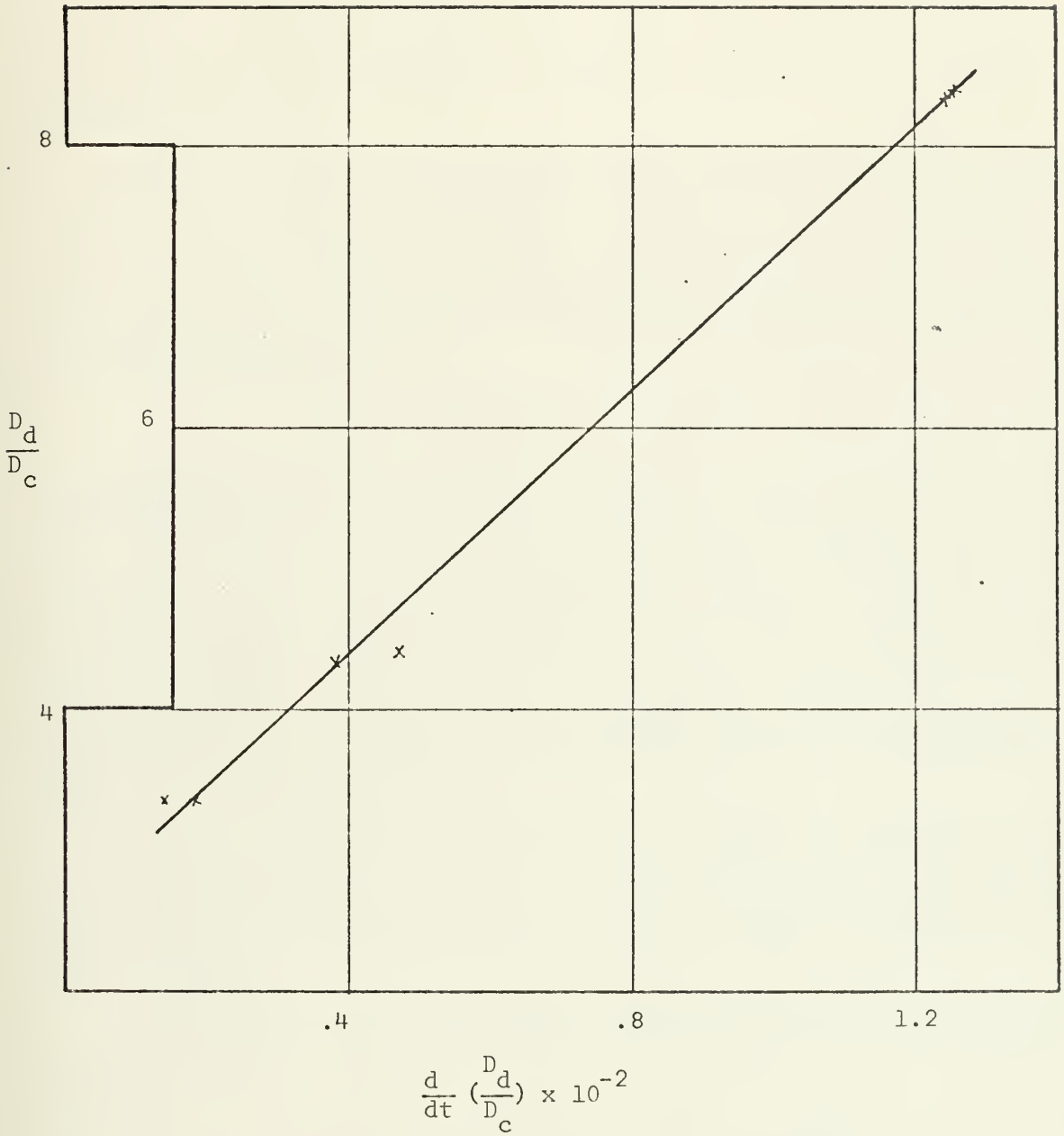

Fig. 14. Ethanol Departure Diameter Ratios vs. Terminal Growth Rates

$$fD_d^{1/2} \approx 0.56\, g^{1/2},$$

the product being independent of fluid properties. All of these formulations predict a lowering of departure diameter with an increase in bubble frequency.

Figure 15, illustrates a log-log plot of the ratio of the equivalent spherical bubble diameter at departure to the cavity diameter versus bubble frequency. The line of best fit drawn through the ethanol data implies the relationship:

$$D_d f^{-.7} = \text{constant}.$$

The separation of the data points for water boiling at low pressures from the best line through the ethanol data points indicates that the constant is a function of fluid properties. The data for ethanol boiling from unheated cavities at medium pressures was neglected. The inordinately low frequency of these bubbles was felt to be caused by growth into a subcooled region.

The major implication of the negative exponent on frequency is the prediction that as bubble frequency increases, the bubble departure size also increases.

A comparison of the Staniszewski formulations, for low pressure ethanol,

$$D_d = 0.625 \sqrt{\frac{2g_c\sigma}{g(\rho_L-\rho_V)}} \left(1 + .855 \frac{dD_d}{dt}\right)$$

and for atmospheric pressure,

$$D_d = .0071\beta \sqrt{\frac{2g_c\sigma}{g(\rho_L-\rho_V)}} \left(1 + .45 \frac{dD_d}{dt}\right),$$

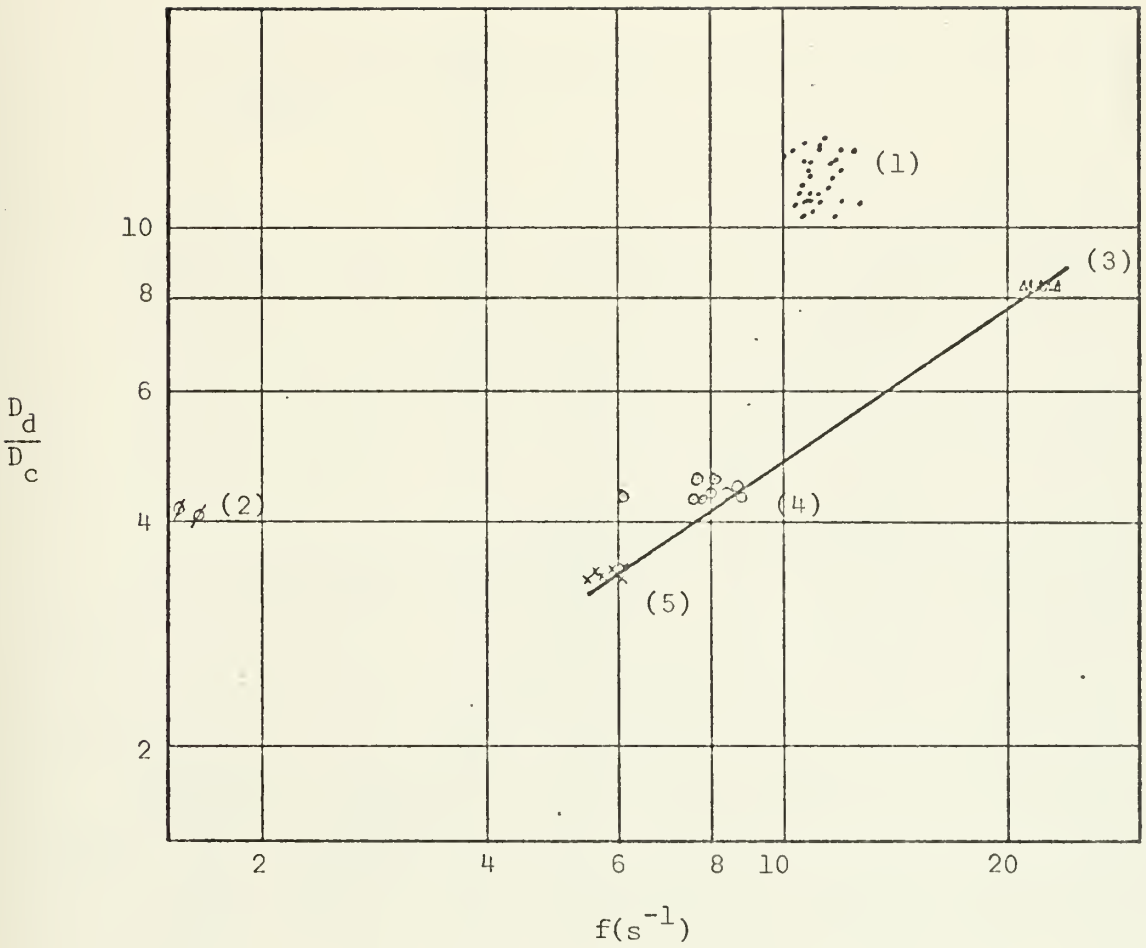

(1) Water at low pressure, 0 and 5W cavity heat

(2) Ethanol medium pressure, 0 cavity heat

(3) Ethanol at low pressure, 9W cavity heat

(4) Ethanol at low pressure, 0 cavity heat

(5) Ethanol at medium pressure, 9W cavity heat

Fig. 15. Departure Diameters vs. Bubble Frequencies

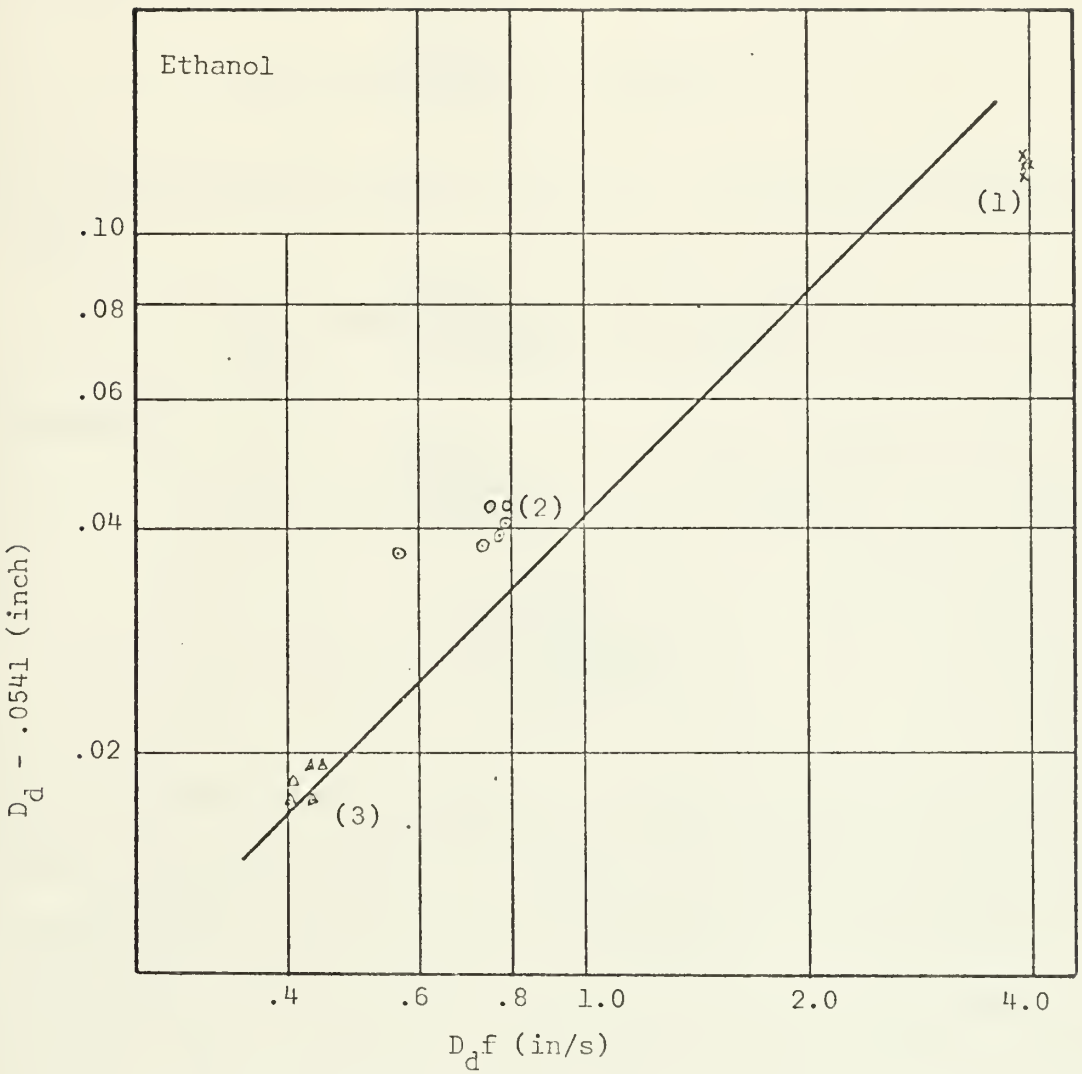

(1) Low pressure, 9W cavity heat

(2) Low pressure, 0 cavity heat

(3) Medium pressure, 9W cavity heat

Fig. 16. Corrected Departure Diameters vs. Frequency-Departure Diameter Products for Ethanol

indicates an increasing dependence upon the dynamic effects, $\frac{dD_d}{dt}$, as pressure is reduced. If $\frac{dD_d}{dt}$ is approximated by $D_d f$, and the Staniszewski equation re-arranged,

$$D_d - .625 \sqrt{\frac{2g_c\sigma}{g(\rho_L-\rho_V)}} = a(D_d f).$$

This relationship is plotted on Fig. 16. It was determined from Fig. 16 that

$$D_d - .625 \sqrt{\frac{2g_c\sigma}{(\rho_L-\rho_V)g}} = .041\ (D_d f).$$

Rearranging

$$D_d = .625 \sqrt{\frac{2g_c\sigma}{g(\rho_L-\rho_V)}}\ (1 + .756\ (D_d f)) \qquad (1)$$

or

$$f = 24.4 \left(1 - \frac{.625\sqrt{\frac{g_c\sigma}{g(\rho_L-\rho_V)}}}{D_d}\right). \qquad (2)$$

Equation (1) indicates the importance of dynamic effects at low pressures, when the $D_d f$ product is of order one. Equation (2) predicts an increasing bubble departure size with increasing bubble frequency, a critical bubble departure size for nucleation and a maximum bubble frequency. The critical bubble departure size for nucleation was thus calculated to be 2.55 cavity diameters. The maximum predicted bubble frequency was 24.4/S. During experimental runs, no bubbles were observed to depart with diameter ratios less than 2.55 and no bubble frequencies greater than 24.4/S were observed. A further point of interest is that the numerator of equation 2,

$$\frac{0.625 \sqrt{\frac{g_c\sigma}{g(\rho_L-\rho_V)}}}{D_d},$$

is the Fritz prediction for the departure diameter. Equation (2) thus predicts Fritz's solution for bubbles of zero frequency.

A physical explanation of the increasing dynamic effects with decreasing pressure may be found in the basic shapes of bubbles growing at a wall at both high and low pressures. At low pressures, rapidly growing bubbles have been observed to grow in a hemispherical fashion, Kosky [14]. Hemispherical growth would result in a net dynamic force countering buoyancy effects. The dynamic force would be expected to delay bubble departure, thus permitting the bubble to attain a greater size before departure. High pressure bubbles generally grow in a spherical manner. As the dynamic forces act to counter radial growth, vertical dynamic forces are partially cancelled through growth on the bubble bottom. Figure 17 illustrates the distributions of these forces.

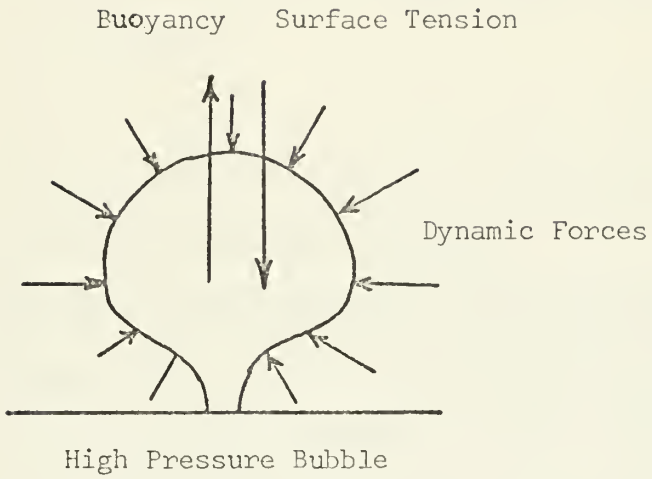

Fig. 17. Force Distributions on High and Low Pressure Bubbles

IV. CONCLUSIONS

1. Bubble growth studies indicate that vapor bubble growth can accurately be described by:

$$D \alpha t^n.$$

The value of n being affected by pressure, cavity heat, fluid, bubble size, and local convection currents.

2. Departure diameters at reduced pressures are more strongly affected by dynamic effects than are the departure diameters at atmospheric and increased pressures.

3. At low pressures bubble departure diameter increases with increasing frequency. It is felt that this behavior is influenced by asymmetric bubble growth at reduced pressures, resulting in a net dynamic force which counters buoyancy forces.

V. RECOMMENDATIONS

1. Investigate the behavior of various fluids, such as Freon and water with wetting agents.
2. Carry out experiments at lower pressures than were utilized in these experiments. Dynamic effects should become more pronounced at lower pressures.
3. Design a boiler that more closely approximates mathematical boundary conditions than did the boiler used herein.
4. Study various cleaning methods necessary to promote wetting.

APPENDIX A - CAVITY AND HEATER CONSTRUCTION

The actual cavity was constructed using .02 inch ID, 3/16 inch OD capillary tubing. A section of the glass was sealed using a torch. Drawing the glass, while hot established the lower cavity geometry. After sealing, the bottom of the cavity section was sawed off 1/16 inch below the cavity bottom. A .10 inch ID, 3/16 inch OD section of tubing was then fused to the bottom of the cavity section. This larger tubing was to be used to house the end of the cavity heater.

At this point, the heater housing was sawed to a 1/8 inch length. The cavity-heater housing assembly was then slipped into a 3/16 ID, 5/16 OD section of Pyrex tubing and fused into the tubing. To insure an optically smooth cavity section, the outer tubing was fused no higher than around the heater housing. As the cavity-heater housing was now attached to its supporting tube, the cavity was cut to the desired length.

The cavity heater was constructed from a 5/8 inch length of nichrome wire, sanded to freely fit in the heater housing. The nichrome wire was then given two coats of GE High Temperature Insulating Varnish and baked according to instructions. After baking, the heater rod was wrapped with four inches of 3 mil nichrome wire to which copper leads had been attached. The wrapped heater was coated with varnish and baked. The finished heater and one lead were slipped into a 1/16 ID glass tube and positioned into the heater housing with the tube. The heater was secured within the housing with a drop of Epoxy glue applied to the tip of the heater rod before positioning. The glass tube used for

positioning was left over the heater, thus separating the copper lead wires and thermally insulating the heater from the cavity supporting tube.

APPENDIX B - TABULATION OF PHYSICAL PROPERTIES

Property	Temp. (°F)	Water	Ethanol
Density	77	62.2	49.0
(lb/ft^3)	190	60.6	
	212	59.9	
Surface	77	71.97	21.9
Tension	190	63.0	
(dynes/cm)	212	58.9	

1 dyne/cm = .000184 lbs/in

Notes:

(a) Physical properties obtained from: The Chemical Rubber Co., Handbook of Tables for Applied Engineering Science, 1970.

(b) Values interpolated from (a).

BIBLIOGRAPHY

1. Staniszewski, B. E., "Nucleate Boiling Bubble Growth and Departure," MIT Report # DSR 7-7673, August 1959.

2. Cole, R., "Bubble Frequencies and Departure Volumes at Subatmospheric Pressures," A.I.Ch.E. Journal, 13, July 1967.

3. Zuber, N., "Hydrodynamic Aspects of Boiling Heat Transfer," Ph. D. Diss., University of California, Los Angeles (1959). AEC Report, AECU 4439, 1959.

4. DuBois, D. R., "Photographic Investigation of Bubble Nucleation from Glass Capillary Tubes," M.S. Thesis, Naval Postgraduate School, Monterey, California, 1967.

5. Sowersby, R. L., "A Photographic Investigation of Bubble Nucleation Characteristics," M.S. Thesis, Naval Postgraduate School, Monterey, California, 1969.

6. Cole, R., and Shulman, H. L., "Bubble Departure Diameters at Subatmospheric Pressures," A.I.Ch.E. Chem. Engr. Prog. Symposium Series, Los Angeles, California, 1966.

7. Griffith, P., "Bubble Growth Rates in Boiling," ASME Transactions, 80, 1958.

8. Plesset, J. J. and Zwick, S. A., "Growth of Vapor Bubbles in Superheated Liquids," Journal of Applied Physics, 25, 1953.

9. Forster, H. K. and Zuber, N., "Growth of a Vapor Bubble in a Superheated Liquid," Journal of Applied Physics, 24, 1953.

10. Zuber, N., "The Dynamics of Vapor Bubbles in Nonuniform Temperature Fields," Int. J. Heat Mass Transfer, 2, 1961.

11. Fritz, W., "Berechnung des Maximalvolumens von Dampfblasen," Physikalische Zeitschrift, 36, January 1935.

12. Jakob, M., Heat Transfer, Vol. 1, Wiley, New York, 1958.

13. McFadden, P. W. and Grassmann, P., "The Relation Between Bubble Frequency and Diameter During Nucleate Pool Boiling," Int. J. Heat Mass Transfer, 5, 1962.

14. Kosky, P. G., "Nucleation Site Instability in Nucleate Boiling," Int. J. Heat Mass Transfer, 11, 1968.

INITIAL DISTRIBUTION LIST

		No. Copies
1.	Defense Documentation Center Cameron Station Alexandria, Virginia 22314	2
2.	Library, Code 0212 Naval Postgraduate School Monterey, California 93940	2
3.	Department of Mechanical Engineering, Code 59 Naval Postgraduate School Monterey, California 93940	1
4.	Assoc. Professor Paul J. Marto, Code 59Mx Department of Mechanical Engineering Naval Postgraduate School Monterey, California 93940	1
5.	ENS. Joel R. Schapira, USN Naval Ship Systems Command (Code 08) Navy Department Washington, D. C. 20360	1

Security Classification

DOCUMENT CONTROL DATA - R & D

(Security classification of title, body of abstract and indexing annotation must be entered when the overall report is classified)

1. ORIGINATING ACTIVITY (Corporate author)	2a. REPORT SECURITY CLASSIFICATION
Naval Postgraduate School Monterey, California 93940	Unclassified
	2b. GROUP

3. REPORT TITLE

Bubble Nucleation from Heated Glass Cavities

4. DESCRIPTIVE NOTES (Type of report and, inclusive dates)

Master's Thesis, June 1972

5. AUTHOR(S) (First name, middle initial, last name)

Joel R. Schapira

6. REPORT DATE	7a. TOTAL NO. OF PAGES	7b. NO. OF REFS
June 1972	53	14

8a. CONTRACT OR GRANT NO.	9a. ORIGINATOR'S REPORT NUMBER(S)
b. PROJECT NO.	
c.	9b. OTHER REPORT NO(S) (Any other numbers that may be assigned this report)
d.	

10. DISTRIBUTION STATEMENT

Approved for public release; distribution unlimited.

11. SUPPLEMENTARY NOTES	12. SPONSORING MILITARY ACTIVITY
	Naval Postgraduate School Monterey, California 93940

13. ABSTRACT

The behavior of bubbles nucleating from a glass cavity was studied using high speed photography. Water and ethanol were used with varying amounts of cavity heat at several subatmospheric pressures.

Bubble growth, departure diameter, and frequency were found to depend on the fluid used, cavity heat, operating pressure and local convection currents. At low pressures, the departure diameter was strongly dependent on dynamic effects. This dependence affected the frequency-departure diameter product such that, contrary to previous high-pressure results, departure diameter increased with increasing bubble frequency.

DD FORM 1 NOV 65 1473 (PAGE 1)

S/N 0101-807-6811

Security Classification

A-31408

14 KEY WORDS	LINK A		LINK B		LINK C	
	ROLE	WT	ROLE	WT	ROLE	WT
bubble nucleation						
subatmospheric boiling						
departure diameters						
bubble growth						
bubble frequency						
nucleate boiling						


4 SEP 73
21542
Thesis
S2485
c.1
Schapira
135327
Bubble nucleation from
heated glass cavities.
4 SEP 73
21542
Thesis
S2485
c.1
Schapira
135327
Bubble nucleation from
heated glass cavities.